Int. J. Electrochem. Sci., 9 **(2014)** 3501 - 3512

International Journal of
ELECTROCHEMICAL
SCIENCE
www.electrochemsci.org

Substituent Effect on Opto-Electrochemical Properties of Thienyl-Derivatized Poly(Phenylcarbazole)S

Lingqian Kong[1,2], *Wei Yang*[3], *Jianzhong Xu*[1,*], *Jinsheng Zhao*[4,*], *Xiuping Ju*[2], *Shengli Li*[2]

[1]College of Chemistry and Environmental Science, Hebei University, Baoding, 071002, P. R. China
[2]Dongchang College, Liaocheng Univesity, Liaocheng, 252059, P. R. China
[3]Engineering Technology Research Institute of China National Petroleum Group, China National Petroleum Corporation (CNPC), 300451, Tianjin, P. R. China
[4]Shandong Key Laboratory of Chemical Energy-storage and Novel Cell Technology, Liaocheng University, 252059, Liaocheng, P. R. China
Corresponding author. Tel: +86-635-8324551; Fax: +86-635-8239001.
[*]E-mail: xjz8112@sina.com; j.s.zhao@163.com

Received: 19 February 2014 / *Accepted:* 20 March 2014 / *Published:* 14 April 2014

Two novel monomers 9-(4-(thiophen-2-yl)phenyl)-9H-carbazole (CBT) and 9-(4-(3-methylthiophen-2-yl)phenyl)-9H-carbazole (CBMT) were synthesized via Suzuki coupling reaction. And, the corresponding polymers PCBT and PCBMT were synthesized electrochemically and characterized in detail. The color of the PCBT was light yellow in its neutral state, and tured to ashy color in the oxidized state, in intermediate states, mahogany color was observed. PCBMT film switches between a colorless state, a gray intermediate state, and a grayish blue oxidized state. The methyl group on the side-chain of the thienyl unites effectively tuned the optical and electronic properties of the polymers, including E_g, HOMO/LUMO, switching properties, etc. The results suggested that the influence of introducing electron-donating group(e.g. methyl group) on polymer's opto-electochemical properties must be considered from the aspects of both the electronic factor and the group's steric effect in polymers.

Keywords: 9-(4-(thiophen-2-yl)phenyl)-9H-carbazole; 9-(4-(3-methylthiophen-2-yl)phenyl)-9H-carbazole; Electrochromic device; Conducting polymer

1. INTRODUCTION

Electrochromism is a phenomenon related to a reversible optical change in absorption or transmittance occurring in materials by a reversible electrochemical process[1]. There are many intrinsically electrochromic materials, such as transiton-metal oxides, inorganic coordination complexes, conjugated polymers, and organic molecules[2–4]. Among them, the conjugated polymers

have several advantages, such as easy processability, high coloration efficiency, fast switching ability, and multiple colors within the same material[5]. Possessing those advantages, conjugated polymers have become one of the main research topics and have quite a number of applications in thin-film transistors[6], sensors[7], polymer light-emitting diodes[8], photovoltaics[9], and electrochromic devices[10–11]. The electrochromism of conjugated polymers is related to the doping-dedoping process, the doping process modifies the polymer electronic structure, producing new electronic states in the band gap, causing color changes[12]. Thus, the electrochromic properties of conducting polymers can be varied over a wide range by controlling the band gap of the polymer via proper choice of heteroaromatic ring and substituents[13].

Polymers derived from various functionalized aromatic derivatives, such as heterocyle-substituted poly(carbazole)s[14], poly(naphthalene)s[15], poly(pyrene)s and poly(fluorene)s[16], have been investigated extensively due to their potential applications in organic light emitting diodes[17], electrochromic devices and photovoltaics[18]. Among these, carbazole and its derivatives have been the subject of investigation because the optical and electrical properties of carbazole can be tuned by different substitution. Generally, fused ring aromatic molecules have more planar geometries so that the materials with fused ring moieties can be expected as promising candidates for optoelectronic device applications[19]. It has reported that modification of the pendant substituent groups is a simple and effective approach for tuning the bandgap in a conjugated polymer[20]. In light of these considerations, it will be of great interest to evaluate the effects of extending the conjugation length of carbazole by electrophilic substitutions and thus modulating the electrochemical and optical properties of the corresponding polymers.

In this report, two kinds of carbazole-based monomers that incorporate thiophene, 3-methylthiophene units are synthesized and electopolymerized. And the substituents variation effect on the optical and electrochemical properties of both the monomers and their corresponding polymers is also studied in detail.

2. EXPERIMENTAL

2.1. Materials

9H-Carbazole, 1,4-dibromobenzene, copper powder, 18-crown-6, trimethylborate ($B(OMe)_3$), 2-bromo-3-methylthiophene, 3,4-ethylenedioxythiophene (EDOT, 98%) and tetrakis(triphenylphosphine)palladium(0) ($Pd(PPh_3)_4$) were all purchased from Aldrich Chemical and used as received. Commercial high-performance liquid chromatography grade acetonitrile (CAN), o-dichlorobenzene (DCB) (Tedia Company, INC., USA) and dichloromethane (DCM, Shanghai Chemical Reagent Company) were used directly without further purification. Sodium perchlorate ($NaClO_4$, Shanghai Chemical Reagent Company, 98%) was dried in a vacuum at 60 ºC for 24 h before use. The precursor 3-methylthiophene-2-boronic acid and 2-thiopheneboronic acid were prepared according to literature method [14]. Other reagents were all used as received without further treatment. Indium-tin-oxide-coated (ITO) glass (sheet resistance : < 10 $\Omega\ \square^{-1}$, purchased from Shenzhen CSG

Display Technologies, China) was successively washed with ethanol, acetone and deionized water in an ultrasonic bath and then dried by a constant stream of N_2.

2.2. Monomers Synthesis

All reactions and manipulations were performed in a nitrogen atmosphere using standard Schlenk techniques. All chromatographic separations were carried out on silica gel.

2.2.1 Synthesis of 9-(4-bromophenyl)-9H-carbazole

A stirred mixture of 9H-carbazole (1.02 g, 6.1 mmol), 1,4-dibromobenzene (2.87 g, 12.2 mmol), K_2CO_3 (3.36 g, 24.5 mmol), Cu powder (0.40 g, 6 mmol) and 18-crown-6 (0.75 g, 3.1 mmol) in DCB (40 ml) was degassed with nitrogen for 1 h. The reaction mixture was then refluxed under a nitrogen atmosphere for another 16 h[21]. The crude mixture was filtered, and the residue was washed with dichloromethane. The combined filtrates were then evaporated to dryness. The product was purified by silica gel flash column chromatography to give the objective compound (1.42 g, 73%) as a white solid. ^{1}H NMR ($CDCl_3$, 400 MHz, ppm): δ=7.26-7.31 (m, 2H), 7.35-7.38(m, 3H), 7.40-7.45 (m, 3H), 7.72 (d, 2H), 8.13 (d, 2H). ^{13}C NMR (CDCl3, δ in ppm): 109.5, 120.2, 120.4, 120.9, 123.5, 126.0, 128.7, 133.1, 136.8, 140.6, detailed synthetic procedures are shown in scheme 1.

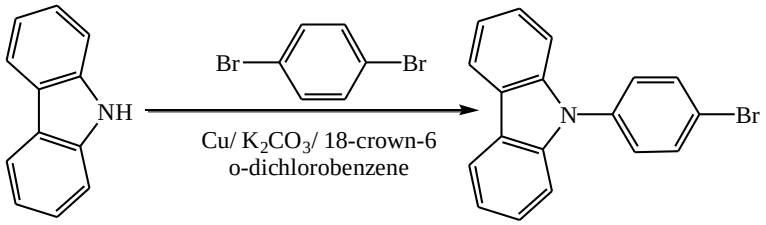

Scheme 1. Synthetic routes of the 9-(4-bromophenyl)-9H-carbazole.

2.2.2 Synthesis of 9-(4-(thiophen-2-yl)phenyl)-9H-carbazole (CBT)

50 mL of anhydrous toluene was added to a mixture of and 2-thiopheneboronic acid. After 10 mL of K_2CO_3 aqueous was added to the stirred mixture, the reaction mixture was degassed with nitrogen for 1 h. Then $Pd(PPh_3)_4$ was added to the mixture. The solution was further refluxed under a nitrogen atmosphere for 24 h[22]. After the reaction solution was cooled to room temperature, the whole mixture was poured into water, and the organic layer was separated and washed with water. The organic extracts were dried over $MgSO_4$ and concentrated by rotary evaporation. After the solvent was evaporated, the crude product was further purified by column chromatography on silica gel to yield the target compound. ^{1}H NMR($CDCl_3$, 400 MHz, ppm): δ=7.12 (t, 1H), 7.28-7.35 (m, 3H), 7.39-7.44 (m, 5H), 7.56 (d, 2H), 7.70 (d, 2H), 8.14 (d, 2H). ^{13}C NMR ($CDCl_3$, δ in ppm): 109.8, 120.0, 120.3, 123.4, 123.6, 125.3, 126.0, 127.2, 127.4, 128.2, 133.5, 136.8, 140.7, 143.4.

2.2.3 Synthesis of 9-(4-(3-methylthiophen-2-yl)phenyl)-9H-carbazole (CBMT)

The procedure of synthesizing the compound was same as the chapter *2.2.1*. There is a subtle difference that, in this process, the reactant 2-thiopheneboronic acid was replaced by 3-methylthiophene-2-boronic acid. The obtained crude product was further purified by a silica gel chromatography; pure product was pale yellow solid. ^{1}H NMR($CDCl_3$, 400 MHz, ppm): δ=2.21 (s, 3H), 7.02 (d, 2H), 7.25-7.40 (m, 3H), 7.40-7.52 (m, 5H), 7.70 (d, 2H), 8.16 (d, 2H). ^{13}C NMR ($CDCl_3$, δ in ppm): 15.4, 111.0, 117.2, 119.6, 120.5, 120.7, 121.7, 125.8, 127.6, 127.41, 130.2, 133.3, 133.6, 138.3, 140.4. The detailed synthetic route is shown in scheme 2.

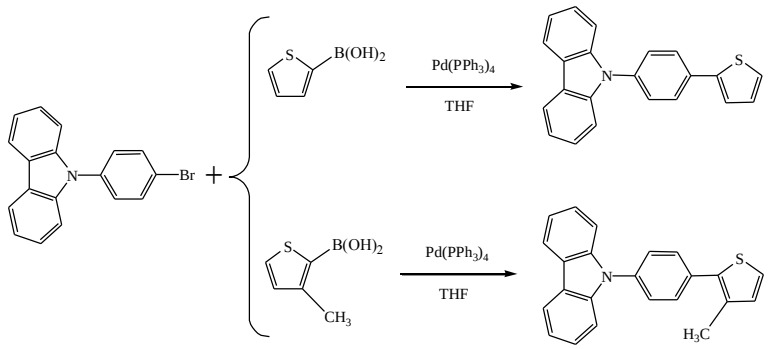

Scheme 2. Synthetic routes of CBT and CBMT.

2.3. Measurements

^{1}H NMR and ^{13}C NMR spectroscopy studies were carried out on a Varian AMX 400 spectrometer and tetramethylsilane (TMS) was used as the internal standard. FT-IR spectra were recorded on a Nicolet 5700 FT-IR spectrometer, where the samples were dispersed in KBr pellets. Electrochemical synthesis and experiments were performed in a one-compartment cell with a CHI 760 C Electrochemical Analyzer under the control of a computer, employing a platinum wire with a diameter of 0.5 mm as working electrode, a platinum ring as counter electrode, and a Ag wire (0.03 V vs. SCE) as pseudo reference electrode. In UV–vis and spectroelectrochemical measurements, solution spectra of the obtained monomers, dissolved in chloroform, as well as the solid state spectra of their thin films deposited on an ITO electrode, were recorded on a Perkin-Elmer Lambda 900 UV–vis–near-infrared spectrophotometer. Moreover, the thickness of the polymer films grown potentiostatically on the ITO electrode was controlled by the total charge passed through the cell. Digital photographs of the polymer films and device cell were taken by a Canon Power Shot A3000 IS digital camera.

2.4. Electrochemical polymerization

Electrochemical polymerization of the monomers was carried out in a ACN/DCM (1:1, by volume) solution of 0.005 M monomer and 0.2 M $NaClO_4$ by repetitive cycling at a scan rate of 100 mV s^{-1}. A platinum wire was used as a counter electrode and Ag wire as a pseudo reference. The

polymers were directly coated onto platinum wire or indium–tin oxide (ITO, < 10 Ω $\square^{-1}$, 0.9 cm × 5 cm) and then the films were rinsed with acetonitrile to remove from electrolyte salt.

2.5. Spectroelectrochemistry

Spectroelectrochemical data were recorded on Shimadzu UV–2550 spectrophotometer connected to a computer. A three-electrode cell assembly was used where the working electrode was an ITO glass, the counter electrode was a stainless steel wire, and an Ag wire was used as pseudo reference electrode. The polymer films for spectroelectrochemistry were prepared by potentiostatically deposition on ITO electrode (the active area: 0.9 cm × 2.0 cm). The thickness of the polymer films grown potentiostatically on ITO is controlled by the total charge passed through the cell. The measurements were carried out in ACN solution containing 0.2 M $NaClO_4$ for CBT and in a mixture of DCM and ACN solution (1:1 by volume) containing 0.2 M $NaClO_4$ for CBMT.

3. RESULTS AND DISCUSSION

3.1. Electrochemical polymerization and characterization

3.1.1 Electrochemical polymerization

Electrochemical polymerization of the monomers were carried out in ACN/DCM (1:1 by volume) solution containing 0.2 M $NaClO_4$, for CBT and CBMT. Fig. 1a shows the cyclic voltammograms (CV) of CBT which has a onset oxidation potential (E_{onset}) at +1.0 V and a peak potential (E_p) at +1.10 V. After the monomer oxidation, a reversible redox couple observed. Compared with CBT, the CBMT (Fig. 1b) has higher E_{onset} (+1.06 V) indicating the methyl groups of CBMT has a larger polymerization steric effect. However, both CMT and CMBT have low polymerization potential.

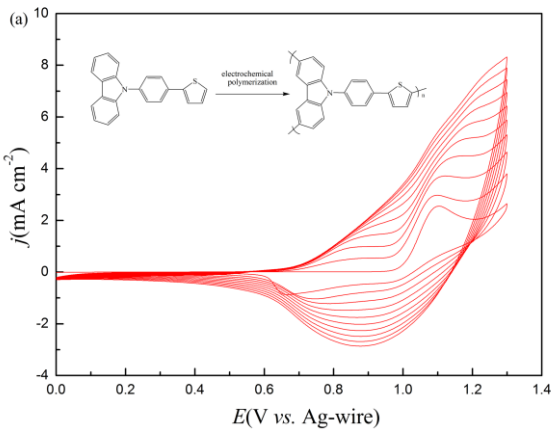

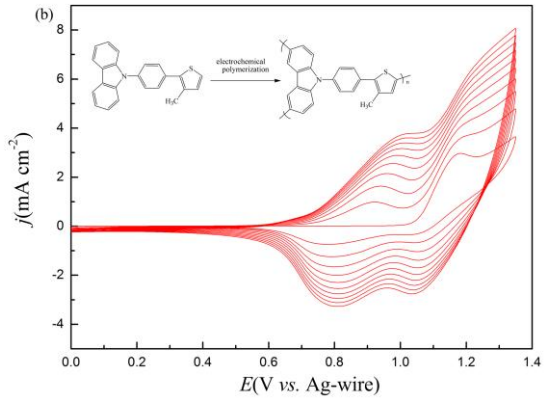

Figure 1. Cyclic voltammogram curves of CBT (a) and CBMT (b) in ACN/DCM solutions containing 0.2 M $NaClO_4$, at a scan rate of 100 mV s^{-1} respectively.

During the repetitive cyclic voltammogram (CV) scans, the current densities of the oxidation/reduction peaks of both CV curves increased, which exhibits the generation of the electroactive conducting polymer on the surface.

3.1.2. Electrochemistry behavior of the polymer films

Fig. 2 shows the electrochemical behavior of the polymer films (prepared on platinum wires by sweeping the potentials three cycles) at different scan rates between 25 and 300 mV s^{-1} in monomer free electrolyte. Fig. 2a shows the CV curves of the poly(9-(4-(thiophen-2-yl)phenyl)-9H-carbazole) (PCBT), the obvious oxidation and reduction peaks are observed at +0.97 V and +0.82 V vs. Ag wire pseudo reference electrode at scan rates 300 mV s^{-1}, respectively. The potential difference between the polymer oxidation and reduction reveals that the redox couple corresponds to one electron reduction for the polymer PCBT[22].

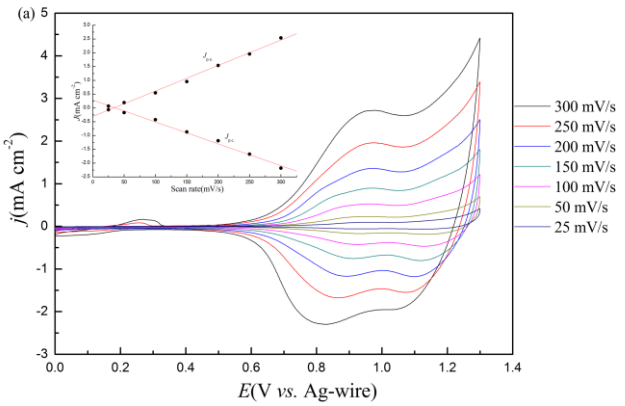

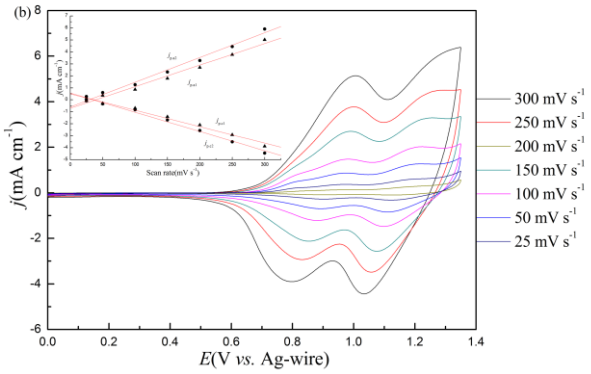

Figure 2. CV curves of the (a) PCBT film and (b) PCBMT film at different scan rates between 25 and 300 mV s^{-1} in the monomer-free $NaClO_4$/ACN/DCM solution, the insert shows the linear relationships between the peak current and the scan rate.

However, the CV curves of the poly(9-(4-(3-methylthiophen-2-yl)phenyl)-9H-carbazole) (PCBMT), displays a wide potential window. From the shapes of cyclic voltammogram, it is predictable that polymer PCBMT has more charge trapping capacity than that of the PCBT. Linear relationships between the peak current and the scan rate designates that the electroactive polymer films were well adhered and the redox processes were non-diffusion controlled[23].

3.1.3 Optical Properties

The UV– vis spectra of CBT and CBMT monomers dissolved in DCM were examined, as shown in Fig. 3. In addition, the UV–vis spectra of neutral state films PCBT and PCBMT on ITO electrode were also studied and also shouwn in Fig.3. In general, the absorption behavior of methyl substituted monomer CBMT and its polymer PCBMT are similarly with that of unsubstituted ones. However, there is an obviously blueshift for both the substituted monomer and polymer. The absorption maximum (λ_{max}) of the monomers CBT and CBMT (upper right inset, Fig. 3) are centered at 304 and 271 nm, respectively. The λ_{max} of CBMT monomer exhibits a 6 nm blueshift compared to that of CBT. From the molecular structures of both monomers, one would expect that the methyl substituted monomer CBMT is less coplanar than that of the none-methyl substituted one, and then the interaction between the methylthiophene and phenylcarbazole is not stronger as that of the thiophene, and finally result in the blue shift of CBMT and its polymer. On the other hand, the λ_{max} of PCBT was observed at about 389 nm, meanwhile, the λ_{max} of PCBMT was observed at about 346 nm. This significant blueshift is attributed to the less longer effective conjugation length of PCBMT than that of PCBT, and the steric effect caused by the methyl group may also act on. Because of these effects, PCBT has a lower band gap value than that of PCBMT. Besides, the CBT and PCBT have higher lying HOMO levels than CBMT and PCBMT, respectively, since polymers with longer effective conjugation length are prone to oxidative doping. Table 1 clearly summarizes the maximum absorption wavelength (λ_{max}), the absorption onsets wavelength (λ_{onset}) and the optical band gap (E_g) of the CBT, CBMT, PCBT, and PCBMT quite clearly.

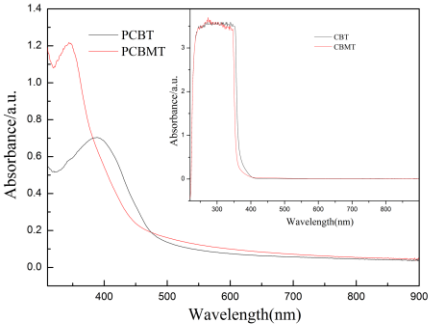

Figure 3. UV–vis absorbtion spectra of PCBT and PCBMT, inset:CBT and CBMT in dichloromethane.

Table 1. The onset oxidation potential (E_{onset}), maximum absorption wavelength (λ_{max}), HOMO and LUMO energy levels and optical band gap (E_g) of CBT, CBMT, PCBT, and PCBMT

Compounds	E_{onset},vs.(Ag-wire) (V)	$\lambda_{max}/\lambda_{onset}$ (nm)	E_g [a] (eV)	HOMO[b] (eV)	LUMO[c] (eV)
CBT	1.00	304/368	3.37	–5.40	–2.03
CBMT	1.06	271/358	3.46	–5.46	–2.00
PCBT	0.65	389/473	2.62	–5.05	–2.43
PCBMT	0.72	346/436	2.84	–5.12	–2.28

[a] Calculated from the low energy absorption edges (λ_{onset}), $E_g = 1240/\lambda_{onset}$

[b] HOMO = –e(E_{onset} + 4.4) (E_{onset} vs. SCE)

[c] Calculated by the subtraction of the optical band gap from the HOMO level

3.1.4. Morphology

The morphologies of polymer films were investigated by scanning electron microscopy (SEM). The PCBT and PCBMT films were prepared by constant potential electrolysis from the solution of 0.2 M $NaClO_4$/ACN/DCM containing relevant monomers on ITO electrodes, respectively, and dedoped before characterization.

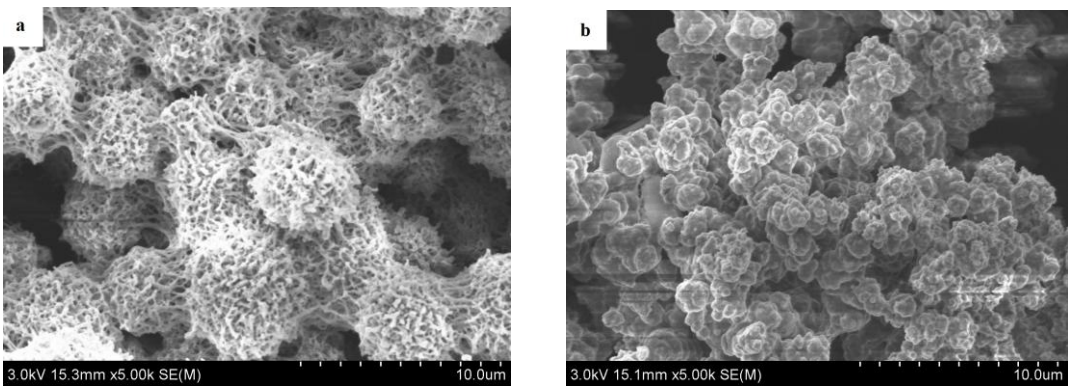

Figure 4. SEM images of PCBT (a) and PCBMT (b) deposited potentiostatically onto ITO electrode.

The SEM images of these polymer films are shown in Fig. 4. The PCBT film presents a loose spongy network structure with much roughens balls (Fig. 4a). However, The PCBMT film exhibits an accumulation state of small globules, and dense holes were also found among the clusters, which is defferent from that of PCBT. These morphologies facilitated the movement of doping anions into and out of the polymer film during doping and dedoping, in good agreement with the good redox activity of PCBT and PCBMT films.

3.2. Electrochromic properties of the polymer films

3.2.1. Spectroelectrochemical properties of the polymer films

Spectroelectrochemistry is a useful method for studying the changes in the absorption spectra and the information about the electronic structures of conjugated polymers as a function of the applied potential difference[24]. The PCBT and PCBMT films were electrodeposited onto ITO (the active area was 0.9 cm × 2.0 cm) with the same polymerization charge of 3.2×10^{-2} C at 1.3 V. The PCBT film was switched between 0 and 1.30 V. At the neutral state, the polymer PCBT film exhibits an absorption band at 387 nm due to the π-π* transition. As shown in Fig. 5a, the intensity of the PCBT π–π* electron transition absorption decreased while two charge carrier absorption bands located at around 561 nm and longer than 900 nm increased dramatically upon oxidation. The appearance of charge carrier bands could be attributed to the evolution of polaron and bipolaron bands. The neutral form of PCBT is light yellow in color. Stepwise oxidation of the polymer shows that the color changes from light yellow to ashy, while mahogany exist at intermediate potentials.

A series of spectra was collected at various potentials ranging from –0.8 V to 1.3 V as shown in Fig. 5b. PCBMT film switches between a colorless state, a gray intermediate state, and a grayish blue oxidized state. Neutral form of PCBMT film gives rise to π–π* absorption band centered at 344 nm. Electrochemical oxidation of the polymer resulted in a decrease in the π–π* transitions and in an increase in the transitions at 774 nm which was characteristic of polarons and bipolarons respectively (Fig. 5b). Although the backbone component is the same, the optical properties of PCBT and PCBMT are different depending on the position of substitution.

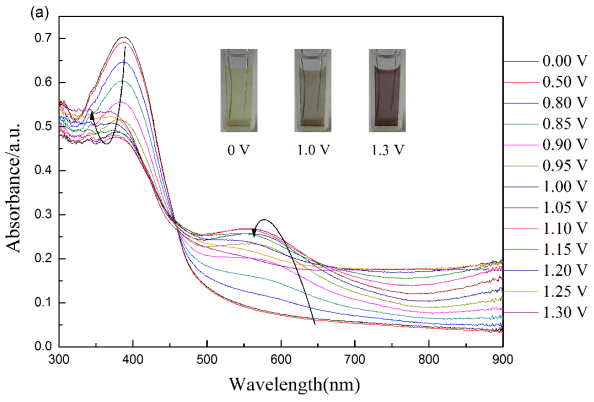

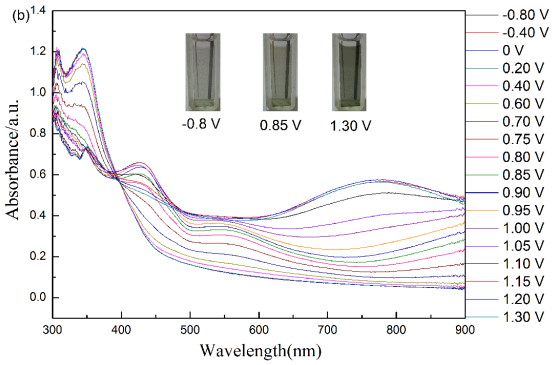

Figure 5. (a) Spectroelectrochemical spectra of PCBT films on ITO electrode as applied potentials between 0 V and 1.30 V in monomer-free 0.2 M $NaClO_4$/ACN/DCM solution (b) Spectroelectrochemical spectra of PCBMT films on ITO electrode as applied potentials between –0.80 V and 1.30 V in monomer-free 0.2 M $NaClO_4$/ACN/DCM solution.

3.2.2. Electrochromic switching of PCBT and PCBMT film in solution

Electrochromic switching studies were carried out to obtain an insight into changes in the optical contrast with time during repeated potential stepping between reduced and oxidized states. One important characteristic of electrochromic materials is the optical contrast (ΔT%), which can be defined as the transmittance difference between the redox states. The optical contrasts after 300 s electrochromic switching were found to be 8.13% at 385 nm and 13.84% at 570 nm for PCBT, 8.41% at 550 nm and 7.99% at 775 nm for PCBMT, as shown in Fig. 6. It is obvious that the PCBT film was better than that of PCBMT film with respect with the electrochromic switching properties including ΔT% and stability.

The PCBMT film shows obvious instability, this phenomenon indicates that the film possess unstable structure, moreover, indicates that the introduction of methyl group into the PCBT molecular chain make the film unstable. It might also indicate that that the methyl group changed the spatial structure of molecular chain, influenced the performance of the conjugated molecules. In a word, the cause of the result is the introducing of methyl group into the molecular chain of CBT, which changed the structure from the molecular level and ultimately affect the electrochromic properties of PCBMT.

Response time, one of the most important characteristics of electrochromic materials, is the necessary time for 95% of the full optical switch (after which the naked eye could not sense the color change) [25]. The optical response time of PCBT was found to be 2.25 s from the reduced to the oxidized state at 570 nm, and the optical response time of PCBMT was found to be 1.20 s from the reduced to the oxidized state at 550 nm. The faster switching response of PCBMT film than that of PCBT film could be ascribed to the faster dopant ion diffusion during the redox process. The moderate optical contrast and response time make PCBT and PCBMT promising electrochromic materials for smart windows.

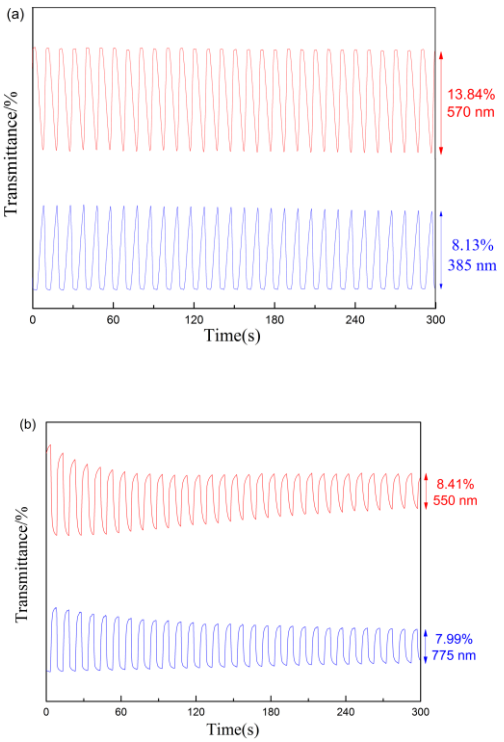

Figure 6. Electrochromic switching, optical absorbance change monitored at (a) 385 nm and 570 nm for PCBT between 0 and 1.30 V, and at (b) 550 and 775 nm for PCBMT between –0.4 and 1.30 V with a same residence time of 4 s.

4. CONCLUSIONS

In conclusion, we have successfully synthesized thiophene and methylthiophene functionalized polyphenylcarbazole. The optical and electrochemical properties of the resulting polymers, such as band gap, redox potentials and energy levels were found to be somewhat different due to the introduction of the methyl group. The electrochemical studies suggested that the introduction of the methyl group into the PCBT molecular chain have increased E_{onset} values ranging from 0.65 V for PCBT to 0.72 V for PCBMT. The optical band gaps (E_g) of the thiophene substituted polyphenylcarbazole (2.62 eV) is lower than that of methylthiophene substituted polymer (2.84 eV). And there is a obviously difference between the two polymers' electrochromic properties. In conclusion, if the substituted group's sterically influence is larger than the electron donor properties, then side groups will damage the conjugate properties of the polymer, thereby affecting its optoelectronic properties.

ACKNOWLEDGEMENTS
The work was financially supported by the China postdoctoral science foundation on the 53th program (2013M530397).

References

1. A. Maier, AR. Rabindranath, B. Tieke, *Adv. Mater*., 21 (2009)959.
2. L. Motiei, M. Lahav, D. Freeman, M.E. van der Boom, *J. Am. Chem. Soc*., 131 (2009) 3468.
3. P.M. Beaujuge, J.R. Reynolds, *Chem. Rev*., 110 (2010) 268.
4. H.J. Yen, H.Y. Lin, G.S. Liou, *Chem. Mater*., 23 (2011) 1874.
5. G. Sonmez, *Chem. Commun*., 42 (2005) 5251.
6. J.J.M. Halls, C.A. Walsh, N.C. Greenham, E.A. Marseglia, R.H. Friend, S.C. Moratti, A.B. Holmes, *Nature*, 376 (1995) 498.
7. D.T. McQuade, A.E. Pullen, T.M. Swager, *Chem. Rev*, 100 (2000) 2537.
8. R.H. Friend, R.W. Gymer, A.B. Holmes, J.H. Burroughes, R.N. Marks, C. Taliani, D.D.C. Bradley, D.A. Dos Santos, *Nature*, 397 (1999) 121.
9. C.J. Brabec, N.S. Sariciftci, J.C. Hummelen, *Adv. Funct. Mater*., 11(2001) 15.
10. O. Turkarslan, M. Ak, C. Tanyeli, I.M. Akhmedov, L. Toppare, *J. Polym. Sci. Part. A: Polym Chem*., 45 (2007) 4496.
11. S. Koyuncu, B. Gultekin, C. Zafer, H. Bilgili, M. Can, S. Demic, I. Kaya, S. Icli, *Electrochim. Acta*., 54 (2009) 5694.
12. Y.A. Udum, Y. Ergun, Y. Sahin, K. Pekmez, A. Yildiz, *J. Mater. Sci*., 44 (2009) 3148.
13. P. Camurlu, E. Şahmetlioğlu, E. Şahin, İM. Akhmedov, C. Tanyeli, L. Toppare., *Thin Solid Films*., 516 (2008) 4139.
14. Y.H. Chen, Y.Y. Lin, Y.C. Chen, J.T. Lin, R.H. Lee, W.J. Kuo, R.J. Jeng, *Polymer*., 52 (2011) 976.
15. P. Data, M. Lapkowski, R. Motyka, J. Suwinski, *Electrochim Acta*., 83 (2012) 271.
16. A.M. Fraind, J.D. Tovar, *J. Phys. Chem. B*., 114 (2010) 3104.
17. A. Yildirima, S. Tarkuc, M. Ak, L. Toppare., *Electrochim. Acta*., 53 (2008) 4875.
18. Y.J. Xing, X.J. Xu, P. Zhang, W.J. Tian, G. Yu, P. Lu, Y.Q. Liu, D.B. Zhu., *Chem. Phys. Lett*., 408 (2005) 169.
19. G.M., Nie, H.J. Yang, J. Chen, Z.M. Bai, *Org. Electron*., 13 (2012) 2167.
20. X.F. Cheng, J.S. Zhao, H.F. Sun, Y.Z. Fu, C.S. Cui, X.X. Zhang, *J. Electroanal. Chem*., 690 (2013) 60–67.
21. S. Koyuncu, B. Gultekin, C. Zafer, H. Bilgili, M. Can, S. Demic, Í. Kaya, S. Icli., *Electrochim Acta*, 54(2009) 5694.
22. B. Yigitsoya, S.M.A. Karimd, A. Balana, D. Barana, L. Toppare, *Synth. Met*., 160 (2010) 2534.
23. B. Yigitsoy, S. Varis, C. Tanyeli, I.M. Akhmedov, L. Toppare, *Electrochim Acta*, 52 (2007) 6561.
24. J. Hwang, J.I. Son, Y.B. Shim., *Sol. Energy. Mater. Sol. Cells*., 94 (2010) 1286.
25. A. Cihaner, F. Algı., *Electrochim. Acta*., 54 (2008) 786.